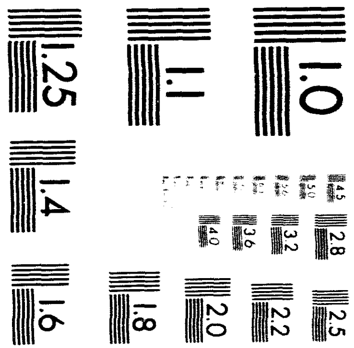

2

SAND93-1725C
Conf-9308911--1

The Structural, Chemical, and Electrical Properties of He-Implantation-Induced Nanocavities in Silicon

C. H. Seager, S.M. Myers, D. M. Follstaedt, H. J. Stein, and W.R. Wampler
Sandia National Laboratories, Albuquerque, N. M. , 87185

Si implanted with He to doses of about 2×10^{16} cm^{-2} and greater and annealed at high temperatures develops a layer of internal nanocavities near the end of the He range. Above an annealing temperature of 700°C, all the implanted He escapes from these implanted samples, and the resultant internal cavity surfaces can be shown to possess a high density of chemically reactive Si dangling orbitals. These structures, in addition to possessing a variety of interesting electronic properties, have recently been shown to hold great promise as getters for removing undesirable impurities from the silicon matrix. Here we describe some of the structural features of these nanocavities and studies which have been used to accurately determine the binding energy of H and Cu to Si atoms at the cavity walls. Recently, we have also demonstrated that these nanocavities capture large densities of majority carriers in n- and p-type silicon. These electrical measurements have demonstrated that the nanocavity electronic states possess both acceptor and donor levels in the Si forbidden gap. The approximate location of these levels has been determined by a variety of different types of capacitance transient spectroscopy.

This work was supported by the United States Department of Energy under Contract DE-AC04-94AL85000.

DISCLAIMER

This report was prepared as an account of work sponsored by an agency of the United States Government. Neither the United States Government nor any agency thereof, nor any of their employees, makes any warranty, express or implied, or assumes any legal liability or responsibility for the accuracy, completeness, or usefulness of any information, apparatus, product, or process disclosed, or represents that its use would not infringe privately owned rights. Reference herein to any specific commercial product, process, or service by trade name, trademark, manufacturer, or otherwise does not necessarily constitute or imply its endorsement, recommendation, or favoring by the United States Government or any agency thereof. The views and opinions of authors expressed herein do not necessarily state or reflect those of the United States Government or any agency thereof.

MASTER

DISTRIBUTION OF THIS DOCUMENT IS UNLIMITED

I. Introduction

It has been recognized for some time that ion implantation of He into Si produces bubbles, and that subsequent annealing at temperatures above 700°C causes the He to diffuse out of the material leaving voids[1]. The empty cavities form a well-defined layer at a depth of about 0.3 μm as seen in the TEM micrograph in Figure 1. Typical cavity size for this implantation and annealing condition is ~ 20 nm, and distinct facetting of the cavity walls can be seen. The walls of these nanocavities are believed to be pristine surfaces, and several of their properties will be discussed in this paper. The dissociation energy of the Si–H surface bond, which has proved inaccessible to ultra-high-vacuum experiments on external Si surfaces, will be accurately determined[2-4], and the transition-metal solute Cu will also be shown to be strongly trapped by these internal surfaces[5]. These results raise the possibility of using cavities for impurity gettering in Si devices. We will also review some recent measurements of the electrical properties of these structures. These latest studies were intended to complement previous UHV photoemission data on external silicon surfaces. Additionally, we sought to determine the effects of cavity-containing layers on the electrical properties of doped Si to facilitate the exploitation these layers in devices for such purposes as impurity gettering.

II. H and Cu -Cavity Interactions

Extensive experimentation has been done at Sandia Laboratories to determine the binding energy of H at internal nanocavity surfaces[2-4]. Figure 2 illustrates that this binding energy is not directly deducible from UHV desorption of H on external cavity surfaces because, although the final state of such a process involves only H-H and H-Si bond energies, the desorption activation energy depends on the energy of a poorly understood intermediate state. This obstacle can be overcome by two separate types of nanocavity-based measurements. In the first Nuclear Reaction Analysis (NRA) was used

to study the equilibrium amount of bonded H at cavity walls at pressures around 1 atm. In a UHV situation such pressures would produce unavoidable contamination of the external surface. In the nanocavity study, however, the surrounding silicon matrix prevents contamination of the nanocavity walls. This measurement yields a value for the Si-H bond energy, E_B of 2.6 ±0.1 eV. The second study of this type involves monitoring the thermal release of H from the nanocavity walls into solution in the silicon lattice, also using NRA. The rate limiting step in this reaction is the promotion of atomic H from internal chemisorption to solution, and the measured rate yielded $E_B = 2.5 \pm 0.2$ eV in excellent agreement with the gas equilibration studies. As a byproduct of these measurements, we were able to use prior UHV desorption results for the desorption activation energy, $E_D \approx$ 2.5 eV, together with our result for E_B, in the equation given in Figure 2 to deduce that the H_2 adsorption activation energy is about 1.8 eV. We also note that FTIR data obtained in conjunction with these experiments[2,4] confirmed the presence of Si-H bonds on the nanocavity surfaces.

Similar experimental techniques were used to estimate the binding energy of Cu on internal cavity surfaces and to compare this with the heat of solution from precipitates of the Cu_3Si phase[5]. The heat of solution for the silicide was obtained by forming Cu_3Si in a near surface layer of a silicon wafer and then observing the transfer of Cu from the silicide to a different layer containing the stronger cavity sinks during annealing. The central idea of these experiments is that the redistribution rate of the Cu is controlled by its solubility in equilibrium with the silicide and by th Cu diffusion coefficient, and the diffusion coefficient can be taken from the literature. This allows the solubility to be determined from the experimental data. The temperature dependence of the solubility then yields the heat of solution.

The Cu_3Si was formed by Cu ion implantation and annealing, and its presence was verified by transmission diffraction. The cavity sinks were located either on the same side of the wafer, at a distance of 0.6 μm from the silicide, or on the opposite side at a distance

of 250 μm. The shorter of these two diffusion distances facilitated measurements at the relatively low temperature of 450°C, while migration over the greater distance was observed at 600°C. The migration of Cu was observed by Rutherford backscattering analysis (RBS), and the accumulation in the cavity sinks is shown as a function of time in Fig. 3. The lines through the data are theoretical fits yielding the heat of solution. The result is 1.7 eV, in good agreement with the published phase diagram.

The binding energy for Cu in the cavities was determined in a very analogous fashion by observing the redistribution of Cu between two cavity layers, one fully occupied initially and the other initially containing no Cu, that were seperated by ~0.4 μm. Under this condition the redistribution proceeds until the fractional occupancies of trap sites are the same in the two layers, and the redistribution rate is governed by the trap binding energy together with the Cu diffusivity. The areal density of redistributed Cu is plotted in Fig. 4 as a function of time at two temperatures, 650 and 700 °C. The curves through the data represent theoretical fits yielding the trap binding energy, 2.2 ±0.2 eV relative to Cu in solution. Thus, nanocavities provide a sink for Cu that is ~0.5 eV stronger than silicide formation.

III Electrical Properties

We anticipate that the dangling Si orbitals on internal cavity surfaces will possess positive, neutral, and negative charge states corresponding to occupation by 0, 1 or 2 electrons. Such states have been seen on clean external Si surfaces[6], Si/SiO_2 interfaces[7-9], grain boundaries[10], and dislocations[11]. Because such ambipolar localized states tend to capture majority carriers, one might anticipate that the resulting charge accumulations will lead to bandbending in the cavity regions which will repel majority carriers at equilibrium. A schematic of the expected charge trapping is shown for n-type Si in Figure 5. A readily identifiable signature of such structures is the substantial impedance they

offer to majority carrier current flow. We have prepared n- and p-type Si wafers with 300 keV He implants and both ohmic and Schottky barrier contacts to look for charging effects of this type[12].

Figures 6 and 7 show the measured zero-bias conductance versus inverse temperature for ohmically contacted samples of this type. In these measurements we forced current to cross the sub-surface nanocavity layer by applying a small potential difference across the front and back ohmic contacts. We see that there is indeed substantial impedance caused by the nanocavity layers, and at least at high temperatures, a temperature dependence consistent with thermionic emission of majority carriers. The expected dependence for the zero-bias conductance under these situations is given by[13]:

$$G = (A^{*}Te/k^{2})\exp((\phi_B+\zeta)/kT) \quad , \qquad (1)$$

where ϕ_B is the electrostatic band bending at the top of the nanocavity-associated electrostatic barrier, ζ is the energy difference between the Fermi level and the conduction band bottom, A* is the Richardson constant, e is the elecronic charge, T is the absolute temp^^rature, and k is the Boltzmann constant. We believe that the weaker temperature dependence seen below ~270K is due to current crossing occasional low spots in the potential barriers which result from the statistical nature of the cavity distribution. High frequency capacitance measurements on these same samples were interpreted to yield the width of the depleted region around the nanocavities using[13]:

$$C_{hf} = A\,\varepsilon/w \quad , \qquad (2)$$

where A is the sample area, ε is the dielectric constant of silicon (1.06×10^{-12} f/cm), and w is a measure of the depletion width surrounding the nanocavities. Figures 8 and 9 show the values of w deduced from our experimental data using Equation 2. We note that the

depletion region around the cavities is of the order of, but somewhat wider than, the nanocavity layer itself.

In addition to these probes of the equilibrium bandstructure around the nanocavities, we also performed transient capacitance measurements on a number of nanocavity samples with ohmic and Schottky contacts. Figure 10 shows the results for electron emission from the upper dangling bond (doubly occupied) level, and Figure 11 shows emission data for holes excited from both localized state levels. These measurements indicate that the upper dangling bond level lies ~ 0.37 eV below the conduction band minimum, and the lower level is ~ 0.17 above the valence band maximum. Using these energy level positions we have simulated the cavity charging with a simple picture in which we allow at most one electron or hole to occupy each cavity, and many of the experimental features that we see can be understood in a semi-quantitative fashion with this approach[12].

IV. Conclusions

Various studies of the chemical and electronic properties of He-implantation-induced nanocavites have been carried out. These structures are extremely chemically reactive and can bind H and transition metal impurities at temperatures above 600°C. For this reason they may provide an attractive alternative to conventional gettering methods in situations where the additional expense of ion implantation can be tolerated. In addition to their unique chemical properties, nanocavities are strong traps for electronic charge and have a profound influence on the nearby Si bandstructure and electronic transport of majority and minority carriers.

References

1. C. C. Griffioen, J. H. Evans, P. C. De Jong, and A. Van Veen, Nucl. Instrum. Meth. B **27**, 417 (1987).
2. S. M. Myers, D. M. Follstaedt, H. J. Stein, and W. R. Wampler, Phys. Rev. B **47**, 13380 (1993).
3. W. R. Wampler, S. M. Myers, and D. M. Follstaedt, Phys. Rev. B **48**, 4492 (1993).
4. H. J. Stein, S. M. Myers, and D. M. Follstaedt, J. Appl. Phys. **73**, 2755 (1993).
5. S. M. Myers, D. M. Follstaedt, and D. M. Bishop, Proc. 17th Inter. Conf. on Defects in Semiconductors, Gmunden, Austria, July 18-23,1993, in press.
6. F. J. Himpsel, Surf. Sci. Reports **12**, 1, (1990).
7. P. J. Caplan, E. H. Poindexter, B. E. Deal, and R. R. Razouk, J. Appl. Phys. **50**, 5487 (1979).
8. E. H. Poindexter, P. J. Caplan, B. E. Deal, and R.R. Razouk, J. Appl. Phys. **52**, 879 (1981).
9. P. M. Lenahan and P. V. Dressendorfer, Appl. Phys. Lett.**41**, 542 (1982).
10. See for example, C. H. Seager, E. L. Venturini, and W. K. Schubert, J. Appl. Phys. **71**, 5059 (1992).
11. V.V. Kveder, A. E. Koshelev, T. R. Mchedlidze, Y. A. Osipyan, and A. Shalynin, Zh. Espk. Teor. Fiz. **95**, 183 (1989).
12. C. H. Seager, S. M. Myers, R. A. Anderson, W. L. Warren, and D. M. Follstaedt, submitted to the Physical Review.
13. W.E. Taylor, N. H. Odell, and H. Y. Fan, Phys. Rev. **88**, 867 (1952).

Figure Captions

Figure 1. <110> cross-sectional TEM micrograph of a silicon sample which has been implanted with 1×10^{17} He/ cm^2 at 30 keV followed by a 900°C ,1 hr. vacuum anneal. Clear evidence of facetting is seen.

Figure 2. A schematic energy diagram for the reaction path between H chemisorbed on silicon and H_2 in vacuum.

Figure 3. The accumulation of Cu at nanocavities, resulting in dissolution of Cu_3Si, as a function of anneal time. Open circles are for an experiment where the cavities were on the opposite side of the wafer from the silicide layer, while the filled circles are data from an experiment where the silicide was on the same side of the wafer as the nanocavities. Theoretical fits are shown as solid lines.

Figure 4. The areal density of Cu transferred from an initially saturated cavity layer to an initially empty cavity layer as a function of anneal time at two temperatures. Solid lines are theory fits using a Cu-cavity binding energy of 2.2 eV.

Figure 5. A schematic representation of the expected bandbending produced by the trapping of electrons at cavity layers in n-type silicon.

Figure 6. Conductance divided by absolute temperature versus inverse temperature for an ohmically contacted n-type Si sample containing a buried layer of He implantation-produced nanocavities. The sample electrode area was 11.6 mm^2.

Figure 7. Conductance divided by absolute temperature versus inverse temperature for an ohmically contacted p-type Si sample containing a buried layer of He implantation-produced nanocavities. The sample electrode area was 11.6 mm^2.

Figure 8. The depletion layer width deduced from 1 MHz capacitance at zero dc bias for an ohmically contacted n-type Si sample containing a buried layer of He implantation-produced nanocavities. The sample electrode area was 11.6 mm^2.

Figure 9. The depletion layer width deduced from 1 MHz capacitance at zero dc bias for a ohmically contacted p-type Si sample containing a buried layer of He implantation-produced nanocavities. The sample electrode area was 11.6 mm^2.

Figure 10. The measured electron emission rate divided by absolute temperature squared deduced from 1 MHz capacitance transients on n-type ohmically contacted Si samples. Filled circles are for data obtained after +1 to 0 volt transitions; Filled squares are for data obtained after -1 to 0 volt transitions. The origin of the lower energy emission process is uncertain, but it is thought to involve emission from P donors located near or on nanocavity surfaces.

Figure 11. Measured hole emission rates divided by absolute temperature squared for ohmically contacted and Schottky barrier p-type samples. The filled circles are deduced from DLTS measurements on Schottky barrier samples, and the open circles are from capacitance relaxation transients measured after majority carrier injection pulses on ohmically contacted samples.

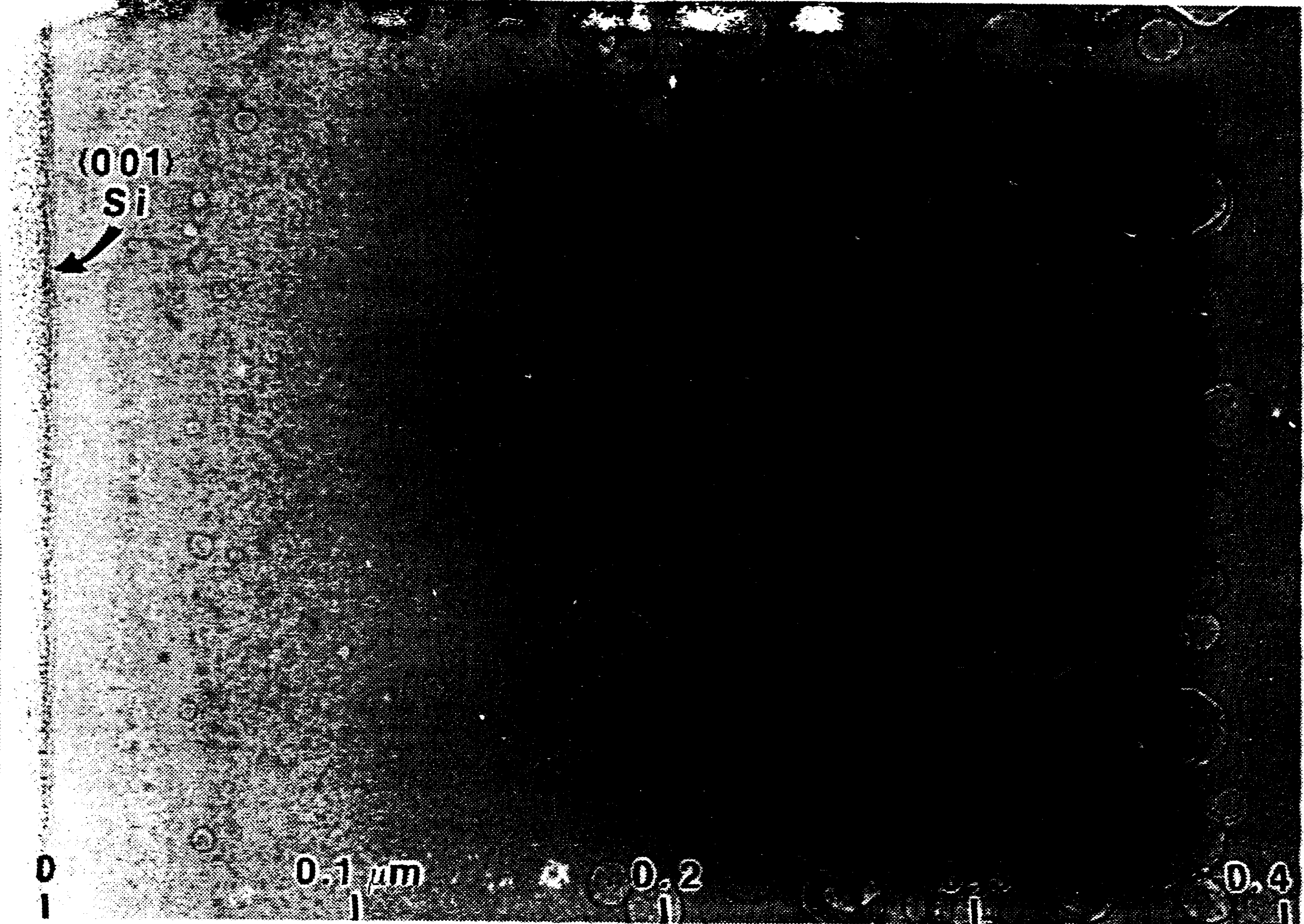

FIG 1

H ENERGETICS ON Si SURFACE

$$E_D = 2\,E_B - E_R + E_A$$

E_D = DESORB ACTIVATION E.
E_B = Si-H BOND ENERGY
E_R = H-H BOND ENERGY
E_A = ADSORB ACTIVATION E.

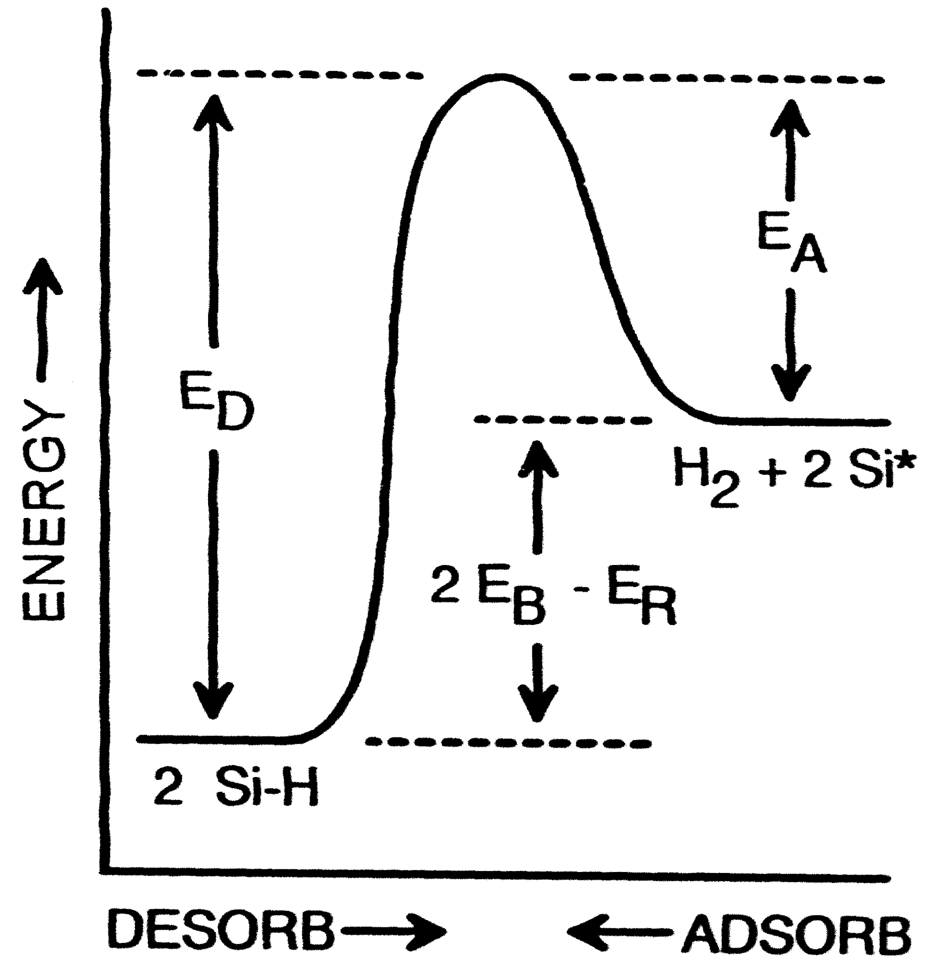

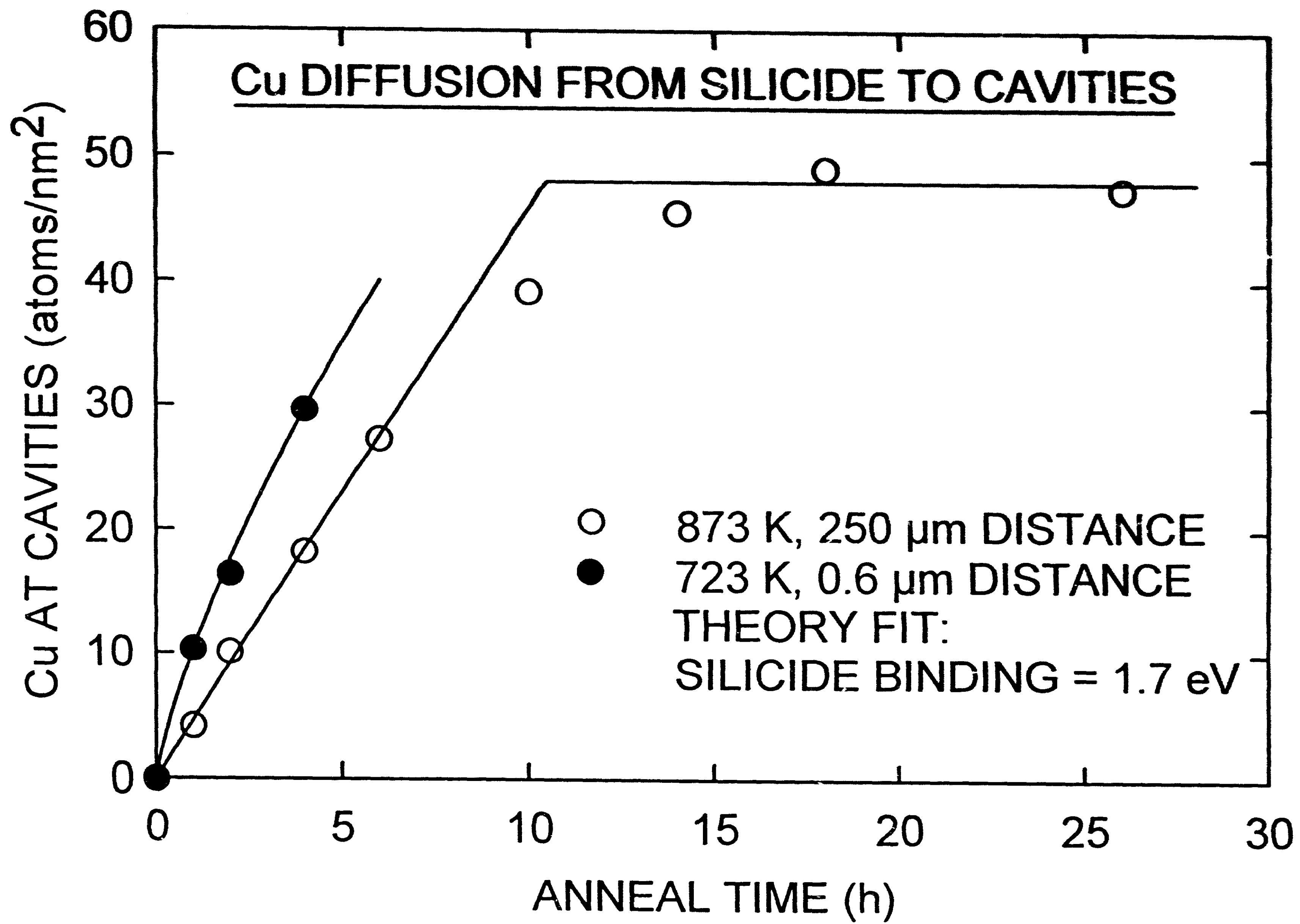
Cu DIFFUSION FROM SILICIDE TO CAVITIES
Cu AT CAVITIES (atoms/nm^2)
60
50
40
30
20
10
0
0
5
10
15
20
25
30
ANNEAL TIME (h)
873 K, 250 μm DISTANCE
723 K, 0.6 μm DISTANCE
THEORY FIT:
SILICIDE BINDING = 1.7 eV

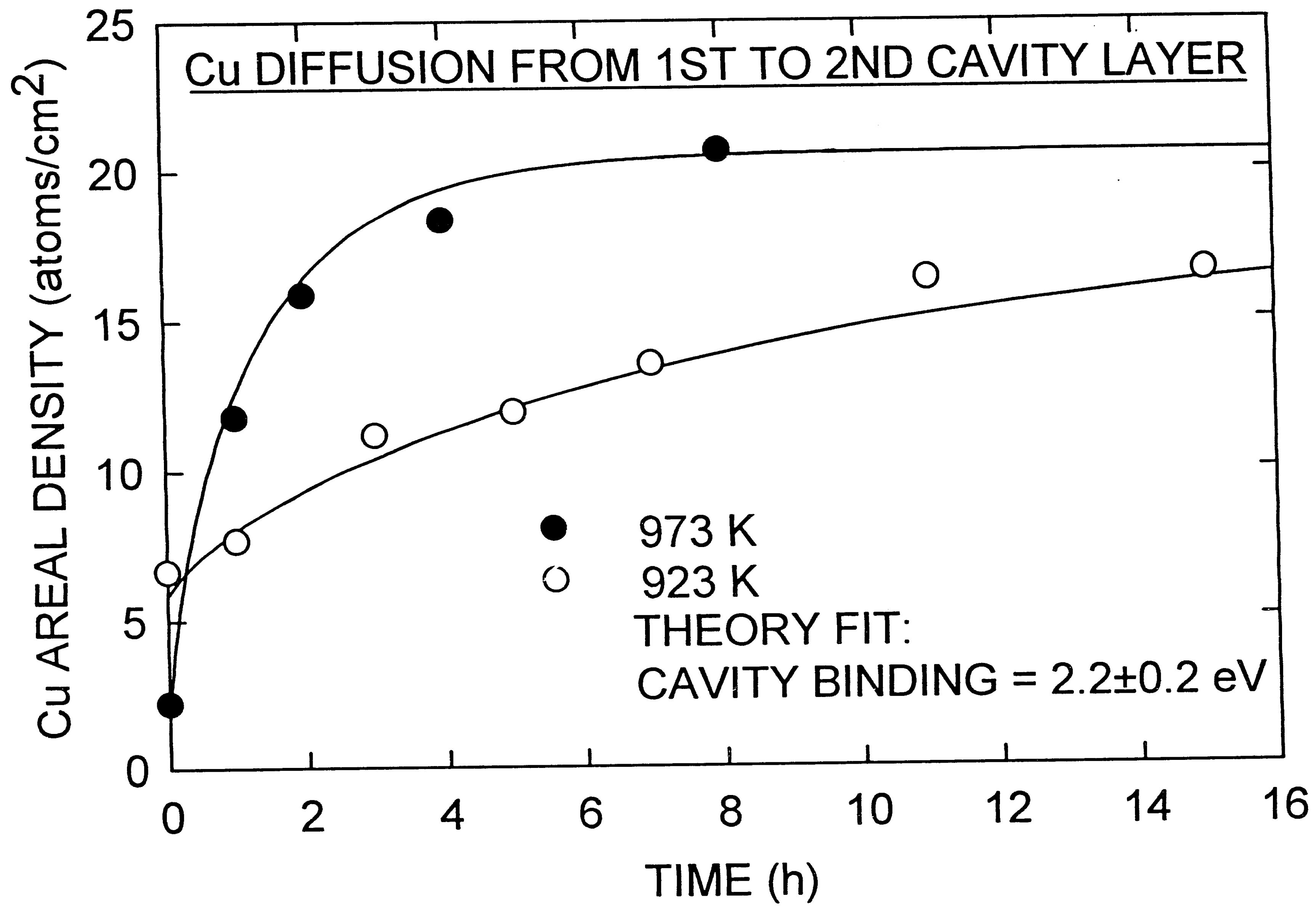

FIG 4

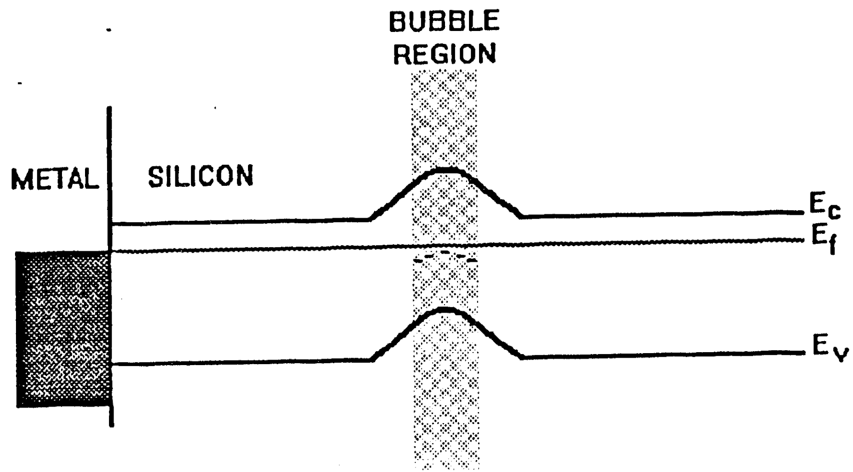
BUBBLE
REGION
METAL
SILICON
E_c
E_f
E_v

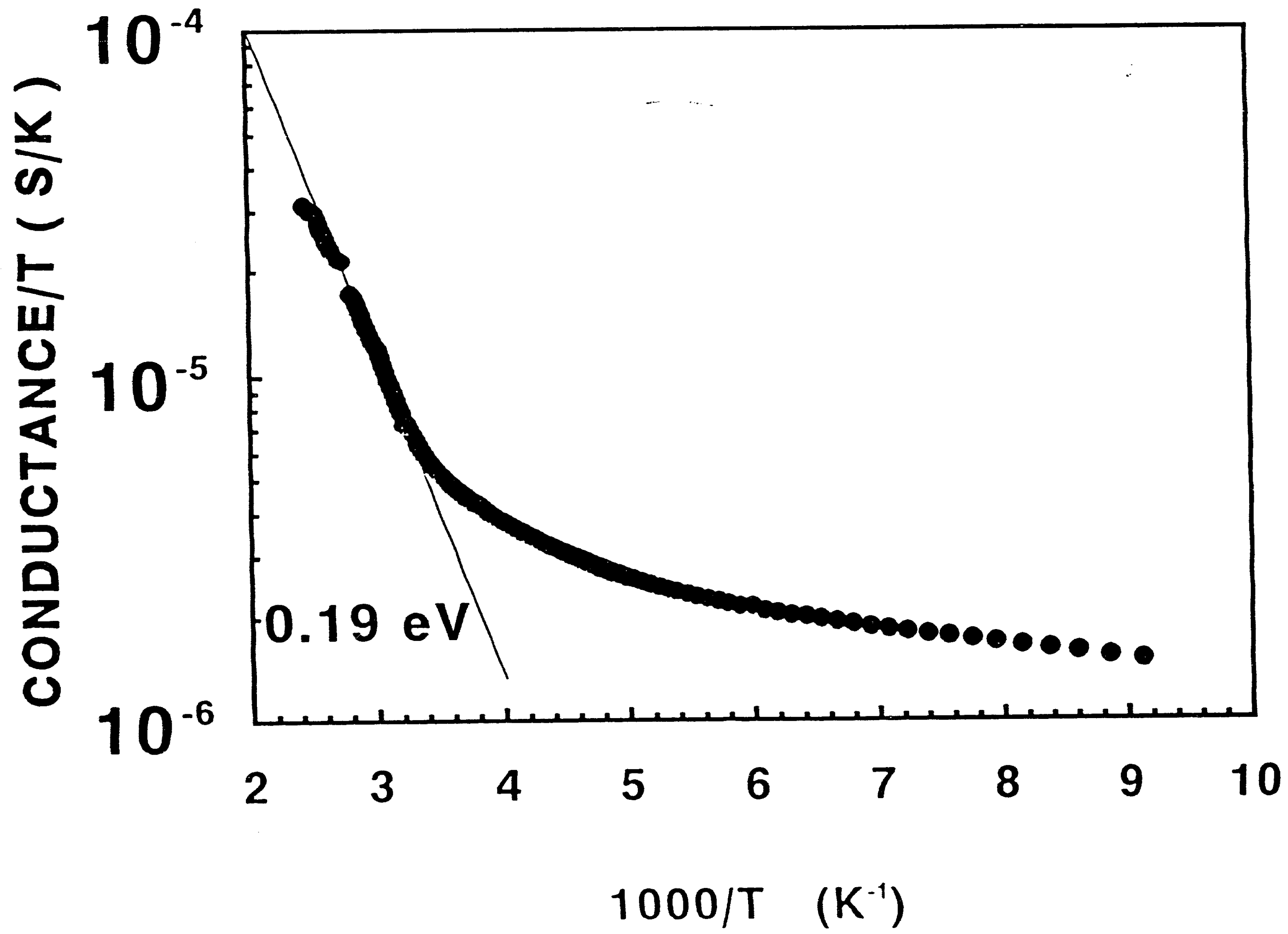

Fig 7

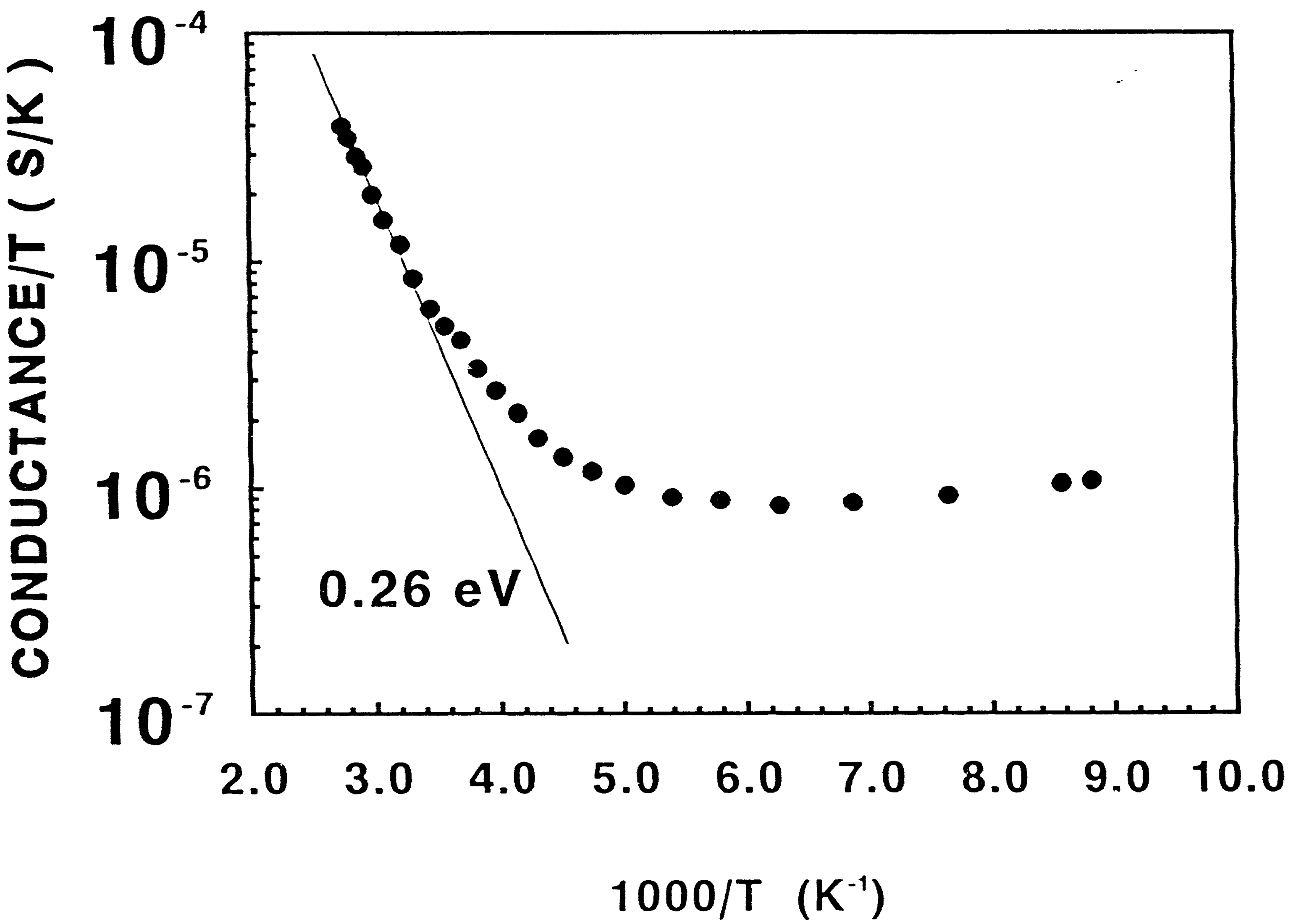

CONDUCTANCE/T (S/K)
10^-4
10^-5
10^-6
10^-7
0.26 eV
2.0
3.0
4.0
5.0
6.0
7.0
8.0
9.0
10.0
1000/T (K^-1)

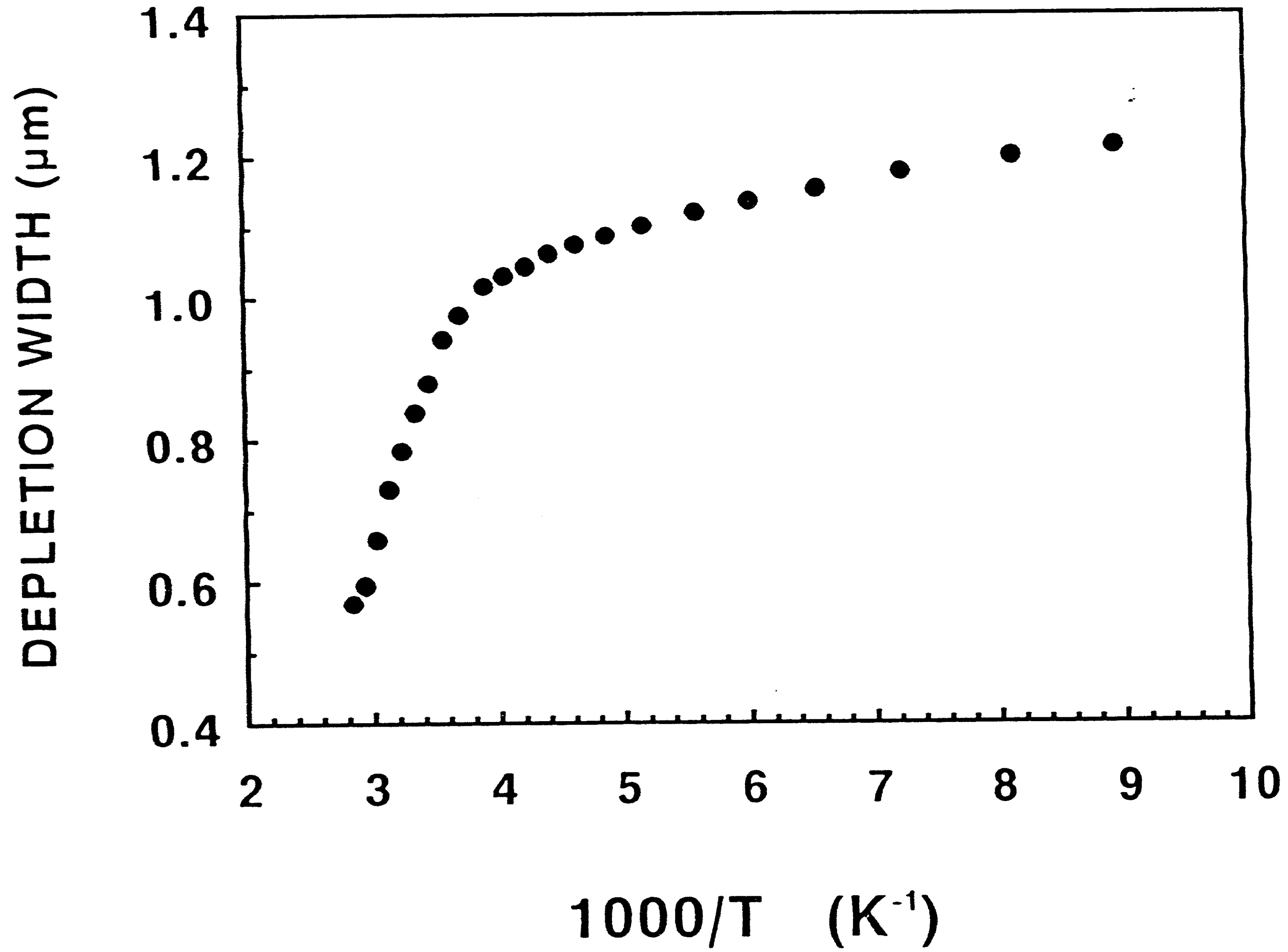

FIG 8

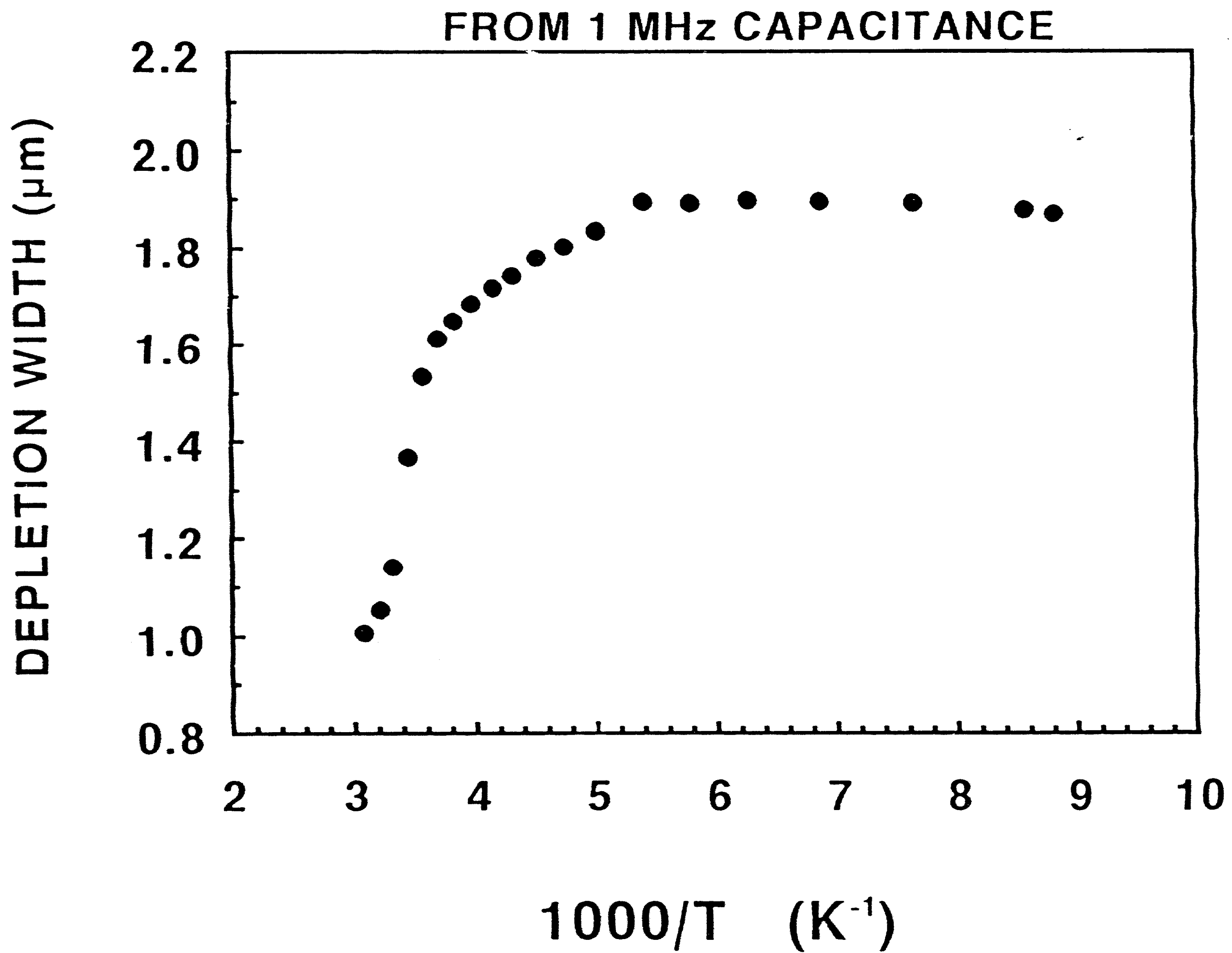

FIG. 4

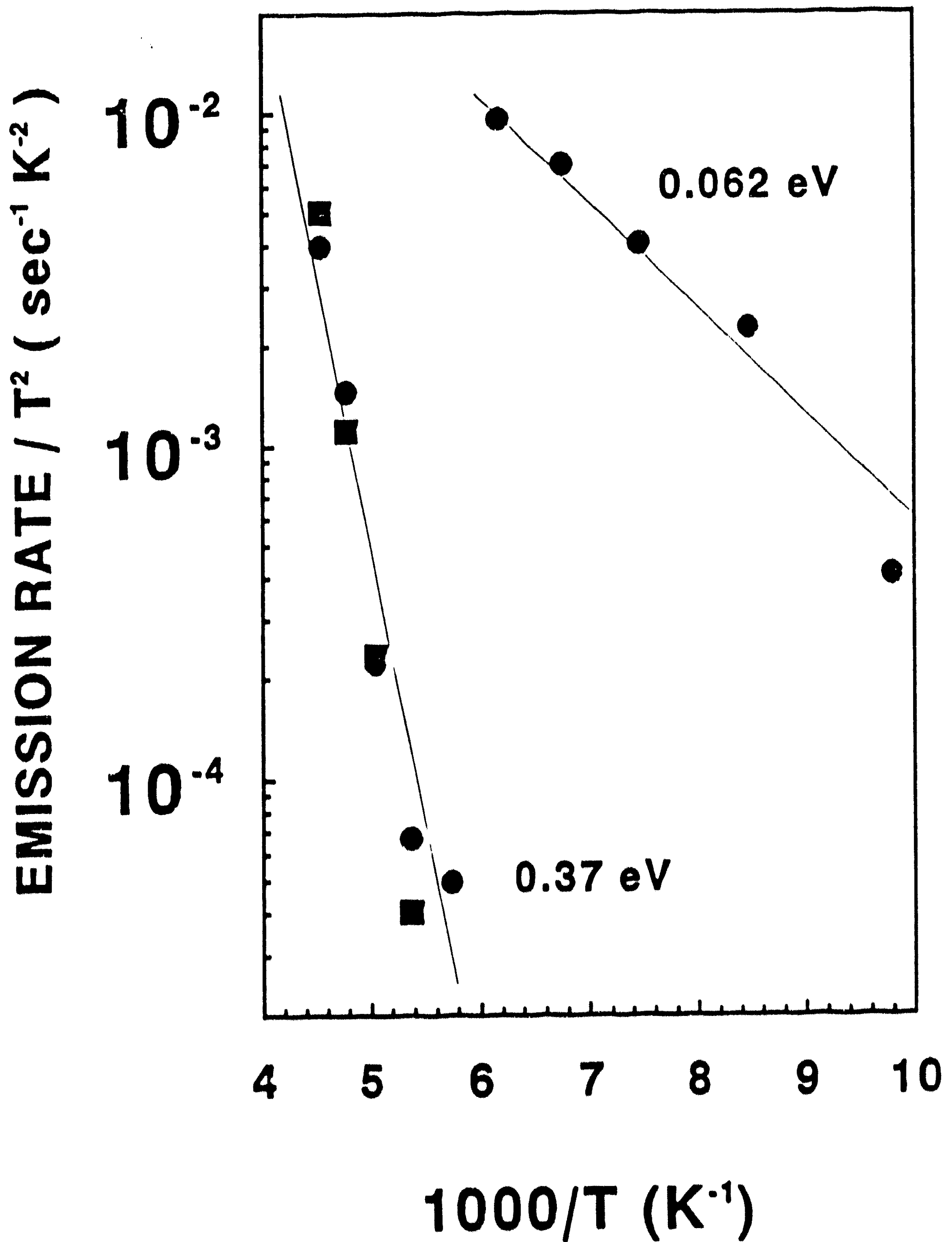

FIG 10

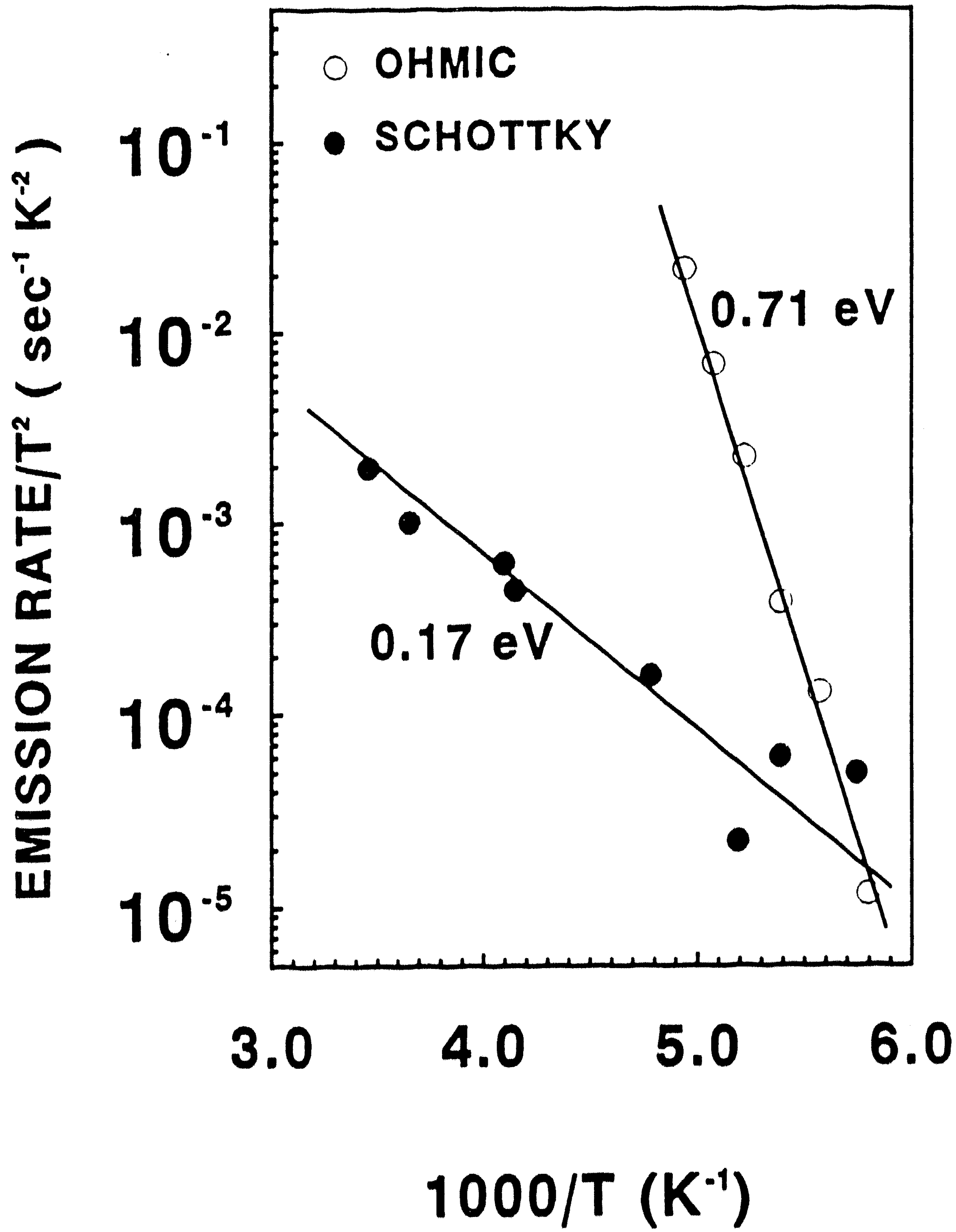

FIG. 1

DATE
FILMED
1 / 12 / 94

END